SCIENCE CHINA
Technological Sciences

September 2010 Vol.53 No.9: 2423–2434
doi: 10.1007/s11431-010-4059-4

Development of an integrated model system to simulate transport and fate of oil spills in seas

WANG JinHua & SHEN YongMing*

State Key Laboratory of Coastal and Offshore Engineering, Dalian University of Technology, Dalian 116023, China

Received October 14, 2009; accepted April 2, 2010

A three-dimensional integrated model is developed for simulating transport and final fate of oil spills in seas. The model contains two main modules, flow and transport-fate modules. The flow module uses an unstructured finite-volume wave-ocean coupling model. Using unstructured meshes provides great flexibility for modeling the flow in complex geometries of tidal creeks, barriers and islands. In the transport-fate module the oil dispersion is solved using a particle-tracking method. Horizontal diffusion is simulated using random walk techniques in a Monte Carlo framework, whereas the vertical diffusion process is solved on the basis of the Langeven equation. The model simulates the most significant processes that affect the motion of oil particles, such as advection, surface spreading, evaporation, dissolution, emulsification and turbulent diffusion as well as the interaction of the oil particles with the shoreline, sedimentation and the temporal variations of oil viscosity, density and surface tension. The model simulates either continuous or instantaneous oil spills, and also other toxic matter. This model has been applied to simulate the oil spill accident in the Bohai Sea. In comparison with the observations, the numerical results indicate that the model is reasonably accurate.

oil-spill modeling, finite-volume method, oil particles, 3-D, unstructured grid

Citation: Wang J H, Shen Y M. Development of an integrated model system to simulate transport and fate of oil spills in seas. Sci China Tech Sci, 2010, 53: 2423–2434, doi: 10.1007/s11431-010-4059-4

1 Introduction

Oil spills in the sea have become common because of growing development of the oil industry, especially seagoing oil transportation. When liquid oil is spilled on the surface of the sea it spreads, forming a thin film, the so-called oil slick. Under surface-wave action and upper layer turbulence, a coherent oil slick will break up into small particles. The oil particles move horizontally on the surface owing to current, wind-induced surface speed, wave drift and horizontal diffusion. Because of sea-surface agitation, some particles entrain and diffuse in the water column. Once in the water column, the displacements of entrained droplets are considered in the three spatial directions. Vertical displacements are due to buoyancy and turbulent diffusion. Figure 1 is a schematic diagram showing these processes [1].

During the last three decades, many investigators have studied the transport and final fate of oil spills based on the trajectory method [2–11]. Among these oil-spill models, many focus on the surface movement of oil spills. There has been little attention given to the hydrodynamic model. Moreover, the hydrodynamic parameters of most spill models are provided by the structured finite difference ocean model. This method is acceptable when the geometry is regular or smooth. When facing an irregular geometry, however, such as the Bohai Strait, with numerous barrier islands and tidal creek complexes, the unstructured grid seems better than the structured grid for capturing suitable physics and reaching a certain accuracy of numerical

*Corresponding author (email: ymshen@dlut.edu.cn)

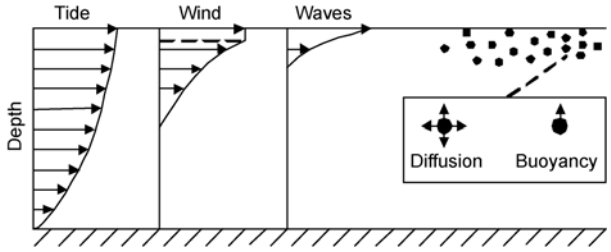

Figure 1 Schematic representation of the mechanisms included in the three-dimensional model [1].

simulation [12]. On the other hand, waves at sea play an important role in the transport and fate of oil particles. Wave motion influences oil behavior in many ways. Wave drift, a netforward movement of waves owing to the not-closed orbitals, transports the oil on the surface, whereas breaking waves disperse and mix the oil with the water. Because of the waves, emulsification of the oil in the water can occur. The oil thickness also depends on the local wave climate. The accurate simulation of the surface wave is therefore important for the oil-spill simulation. Considering the importance of these processes it is necessary to develop a robust oil-spill-simulation system that can provide accurate hydrodynamic parameters, such as waves, ocean currents and turbulence even in an area of complex geometries.

In this paper, a three-dimensional oil-spill transport and fate model, based on the Lagrangian discrete particle algorithm, is developed to simulate the processes of advection, spreading, turbulent diffusion, evaporation, emulsification and dissolution. Horizontal-plane dispersion is calculated on the basis of the random walk technique, whereas vertical particle movements are taken into account on the basis of the Langeven equation and buoyancy effect in the following model. To represent the structure of coastal currents more accurately, a three-dimensional (3-D) unstructured finite-volume ocean-wave coupled model is developed. This is the first time, to our knowledge, that a 3-D, unstructured-grid, primitive-equation, finite-volume ocean-wave model is coupled to provide hydrodynamic parameters required by a transport-fate module. An application of the developed model to simulate the oil-spill accident in the Bohai Sea is also presented.

2 Mathematical model

The model consists of two main modules: flow module and transport-fate module. The overall structure of the model is shown in Figure 2. The flow module, an unstructured finite-volume wave-current coupled model is described first. Next, the transport-fate module is presented.

2.1 Flow module

Since the water current affects both the advection and the spreading of an oil slick, it is necessary to determine the distribution of both the magnitude and the direction of the current. Thus, a parallel, unstructured grid, finite-volume, ocean-wave coupled model is developed for this purpose.

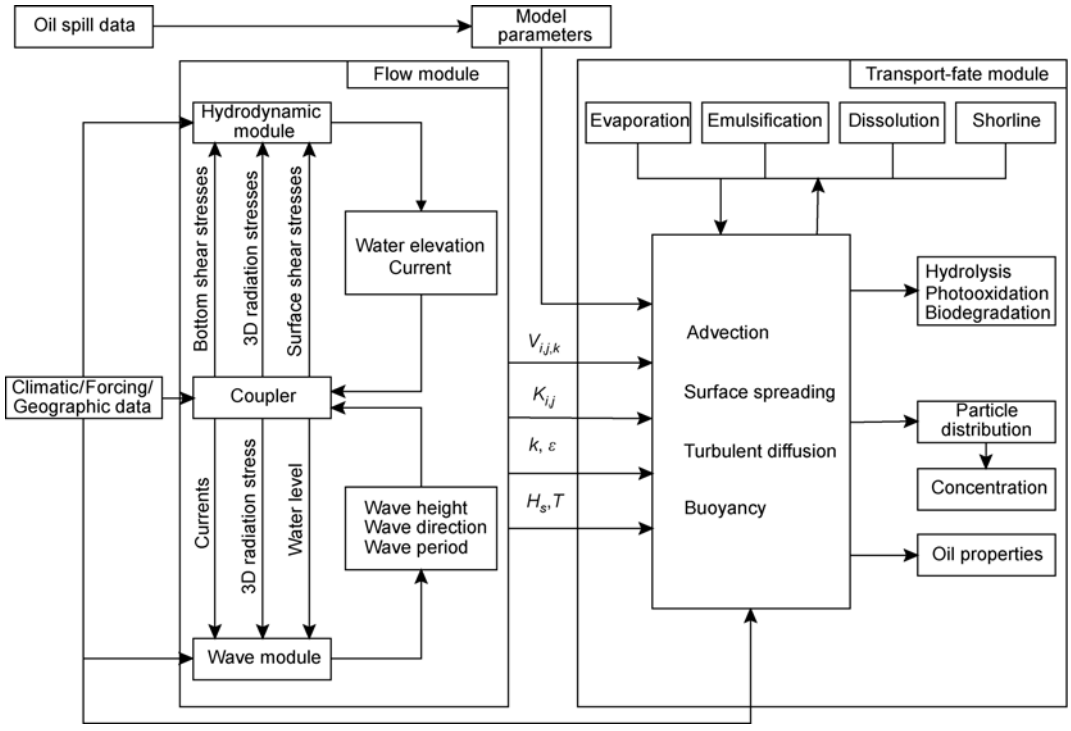

Figure 2 Flow diagram of the computation process in the integrate model system.

2.1.1 Basic equations of the hydrodynamic model

A sigma coordinate is used for the vertical coordinate and the horizontal grid uses a non-overlapped unstructured grid. The momentum equations are

$$\frac{\partial UD}{\partial t}+\frac{\partial U^2D}{\partial x}+\frac{\partial UVD}{\partial y}+\frac{\partial V\omega}{\partial \varsigma}+\frac{gD^2}{\rho_0}\int_{\varsigma}^{0}\left[\frac{\partial \rho}{\partial x}-\frac{\varsigma}{D}\frac{\partial D}{\partial x}\frac{\partial \rho}{\partial \varsigma}\right]\mathrm{d}\varsigma - fVD+gD\frac{\partial \eta}{\partial x}=\frac{\partial}{\partial \varsigma}\left[\frac{K_\mathrm{m}}{D}\frac{\partial U}{\partial \varsigma}\right]+\frac{\partial}{\partial x}\left[2A_\mathrm{m}H\frac{\partial U}{\partial x}\right] +\frac{\partial}{\partial y}\left[A_\mathrm{m}H\left(\frac{\partial U}{\partial y}+\frac{\partial V}{\partial x}\right)\right]+R_x, \tag{1}$$

$$\frac{\partial VD}{\partial t}+\frac{\partial UVD}{\partial x}+\frac{\partial V^2D}{\partial y}+\frac{\partial V\omega}{\partial \varsigma}+\frac{gD^2}{\rho_0}\int_{\varsigma}^{0}\left[\frac{\partial \rho}{\partial y}-\frac{\varsigma}{D}\frac{\partial D}{\partial y}\frac{\partial \rho}{\partial \varsigma}\right]\mathrm{d}\varsigma + fUD+gD\frac{\partial \eta}{\partial y}=\frac{\partial}{\partial \varsigma}\left[\frac{K_\mathrm{m}}{D}\frac{\partial V}{\partial \varsigma}\right]+\frac{\partial}{\partial y}\left[2A_\mathrm{m}H\frac{\partial V}{\partial y}\right] +\frac{\partial}{\partial x}\left[A_\mathrm{m}H\left(\frac{\partial U}{\partial y}+\frac{\partial V}{\partial x}\right)\right]+R_y, \tag{2}$$

$$\frac{\partial p}{\partial \varsigma}+\rho gD=0. \tag{3}$$

With continuity as

$$\frac{\partial DU}{\partial x}+\frac{\partial DV}{\partial y}+\frac{\partial \omega}{\partial \varsigma}+\frac{\partial \eta}{\partial t}=0, \tag{4}$$

and scalar transport

$$\frac{\partial DC}{\partial t}+\frac{\partial UDC}{\partial x}+\frac{\partial VDC}{\partial y}+\frac{\partial \omega DC}{\partial \varsigma}=\frac{1}{D}\frac{\partial}{\partial \varsigma}\left(K_\mathrm{h}\frac{\partial C}{\partial \varsigma}\right) +\frac{\partial}{\partial x}\left[A_\mathrm{h}H\frac{\partial C}{\partial x}\right]+\frac{\partial}{\partial y}\left[A_\mathrm{h}H\frac{\partial C}{\partial y}\right]+C_\mathrm{source}, \tag{5}$$

where U and V are the components of velocity in the horizontal (x and y); f is the Coriolis parameter; ω is the velocity component normal to sigma surfaces; the vertical sigma coordinates $(z-\eta)/D$ range from $\varsigma=-1$ at the bottom to $\varsigma=0$ at the free surface; z is the vertical coordinate positive upwards with z=0 at mean sea level; η is the wave-averaged free-surface elevation; D is the total water depth $D=H+\eta$; H is the depth below mean sea level of the sea floor; p is the pressure; ρ and ρ_0 are total and reference densities for seawater; g is acceleration due to gravity; K_m is the vertical eddy viscosity coefficient and K_h is the thermal vertical eddy diffusion coefficient; A_m and A_h are the horizontal eddy and thermal diffusion coefficients, respectively, and they are determined using a Smagorinsky eddy parameterization method; C represents a tracer quantity (for example, salt, temperature); C_source are tracer source/sink terms (e.g. Temperature, Salinity); R_x, R_y are radiation-stress terms caused by surface wave [13]:

$$\begin{cases} R_x=-D\left(\dfrac{\partial S_{xx}(\varsigma)}{\partial x}+\dfrac{\partial S_{xy}(\varsigma)}{\partial y}\right)+\varsigma\left(\dfrac{\partial D}{\partial x}\dfrac{\partial S_{xx}}{\partial \varsigma}+\dfrac{\partial D}{\partial y}\dfrac{\partial S_{xy}}{\partial \varsigma}\right), \\ R_y=-D\left(\dfrac{\partial S_{yx}(\varsigma)}{\partial x}+\dfrac{\partial S_{yy}(\varsigma)}{\partial y}\right)+\varsigma\left(\dfrac{\partial D}{\partial x}\dfrac{\partial S_{yx}}{\partial \varsigma}+\dfrac{\partial D}{\partial y}\dfrac{\partial S_{yy}}{\partial \varsigma}\right), \end{cases} \tag{6}$$

where

$$\begin{cases} S_{xx}(\varsigma)=E_\mathrm{T}\dfrac{k[\cosh 2k(1+\varsigma)D+1]}{\sinh 2kD}\cos^2\bar{\theta}+E_D -E_\mathrm{T}\dfrac{k[\cosh 2k(1+\varsigma)D-1]}{\sinh 2kD}, \\ S_{yy}(\varsigma)=E_\mathrm{T}\dfrac{k[\cosh 2k(1+\varsigma)D+1]}{\sinh 2kD}\sin^2\bar{\theta}+E_D -E_\mathrm{T}\dfrac{k[\cosh 2k(1+\varsigma)D-1]}{\sinh 2kD}, \\ S_{xy}(\varsigma)=S_{yx}(\varsigma)=E_\mathrm{T}\dfrac{k[\cosh 2k(1+\varsigma)D+1]}{\sinh 2kD}\sin\bar{\theta}\cos\bar{\theta}, \end{cases} \tag{7}$$

where $\bar{\theta}=\tan^{-1}\int_{-\pi}^{\pi}E_\theta\sin\theta\mathrm{d}\theta/\int_{-\pi}^{\pi}E_\theta\cos\theta\mathrm{d}\theta$ is the dominant wave direction relative to the eastward direction; $k_\alpha=k(\cos\bar{\theta},\sin\bar{\theta})$ is the wave number vector and $k=|k_\alpha|$; E_T is the total kinematic wave energy per unit surface area; a modified delta function E_D is equal 0, if $\varsigma\neq 0$ and $\int_{-1}^{0}E_D D\mathrm{d}\varsigma=E/2$.

These equations are closed by parameterizing the Reynolds stresses and turbulent tracer fluxes by solving the turbulent kinetic energy and turbulent macro scale equations

$$\frac{\partial q^2D}{\partial t}+\frac{\partial Uq^2D}{\partial x}+\frac{\partial Vq^2D}{\partial y}+\frac{\partial \omega q^2}{\partial \varsigma}=\frac{\partial}{\partial \varsigma}\left[\frac{K_q}{D}\frac{\partial q^2}{\partial \varsigma}\right] +\frac{2K_\mathrm{m}}{D}\left[\left(\frac{\partial U}{\partial \varsigma}\right)^2+\left(\frac{\partial V}{\partial \varsigma}\right)^2\right]+2\left(\tau_{px}\frac{\partial U}{\partial \varsigma}+\tau_{py}\frac{\partial V}{\partial \varsigma}\right) -\frac{2Dq^3}{B_1 l}+\frac{2g}{\rho_0}K_\mathrm{h}\frac{\partial \tilde{\rho}}{\partial \varsigma}+\frac{\partial}{\partial x}\left(DA_\mathrm{h}\frac{\partial q^2}{\partial x}\right) +\frac{\partial}{\partial y}\left(DA_\mathrm{h}\frac{\partial q^2}{\partial y}\right), \tag{8}$$

$$\frac{\partial q^2lD}{\partial t}+\frac{\partial Uq^2lD}{\partial x}+\frac{\partial Vq^2lD}{\partial y}+\frac{\partial \omega q^2l}{\partial \varsigma}=\frac{\partial}{\partial \varsigma}\left[\frac{K_q}{D}\frac{\partial q^2l}{\partial \varsigma}\right] +E_1 l\left(\frac{K_\mathrm{m}}{D}\left[\left(\frac{\partial U}{\partial \varsigma}\right)^2+\left(\frac{\partial V}{\partial \varsigma}\right)^2\right]+\left(\tau_{px}\frac{\partial U}{\partial \varsigma}+\tau_{py}\frac{\partial V}{\partial \varsigma}\right) +E_3\frac{g}{\rho_0}K_\mathrm{h}\frac{\partial \tilde{\rho}}{\partial \varsigma}\right)-\frac{Dq^3}{B_1}\tilde{W}+\frac{\partial}{\partial x}\left(DA_\mathrm{h}\frac{\partial q^2l}{\partial x}\right) +\frac{\partial}{\partial y}\left(DA_\mathrm{h}\frac{\partial q^2l}{\partial y}\right), \tag{9}$$

where $L^{-1}=(\eta-z)^{-1}+(H+z)^{-1}$; $\tilde{W}=1+E_2 l^2/(\kappa L)^2$ is the wall proximity function, k=0.4 is the von Karman constant; E_1, E_3 and B_1 are close constant of the mode; K_{m} is the vertical eddy viscosity coefficient; K_q is the vertical eddy diffusion coefficient of the turbulent kinetic energy; $\tilde{W}=1+E_2 l^2/(\kappa L)^2$ is a wall proximity function where $L^{-1}=(\eta-z)^{-1}+(H+z)^{-1}$; $q^2/2$ is the turbulence kinetic energy; $\partial\tilde{\rho}/\partial\varsigma=\partial\rho/\partial\varsigma-c_{\mathrm{s}}^{-2}\partial p/\partial\varsigma$, c_{s} is sound velocity; l is the turbulence length scale; τ_p is the pressure stress [14]; turbulent close parameters (K_{m}, K_{h}, K_{q}) have been given by Blumberg and Mellor [15].

2.1.2 *Basic equations of wave model*

The modification of the momentum equations to include the effects of surface waves requires information on basic wave properties such as wave-energy, propagation direction, and wavelength. Other algorithms such as the bottom boundary modules and turbulence sub models may also require wave information such as wave period, bottom orbital velocity, and wave-energy dissipation rate. Therefore, an unstructured grid, finite-volume wind-wave model is developed inspired by Mellor [16]. The basic equations are as follows:

$$\frac{\partial E_\theta}{\partial t}+\frac{\partial}{\partial x_\alpha}\left[(\overline{c}_{g\alpha}+\overline{u}_{\mathrm{A}\alpha})E_\theta\right]+\frac{\partial}{\partial\theta}\left[\overline{c}_\theta E_\theta\right]+\int_{-1}^{0}\overline{S}_{\alpha\beta}\frac{\partial U_\alpha}{\partial x_\beta}D\mathrm{d}\varsigma=S_{\theta\mathrm{in}}-S_{\theta\mathrm{Sdis}}-S_{\theta\mathrm{Bdis}}. \tag{10}$$

The horizontal coordinates are denoted by x_α=(x, y). The over bars represent spectral averages. The first two terms on the left of eq. (10) determine the propagation of wave energy in time and horizontal space whereas the third term is the refraction term accounting for the change in direction of wave energy propagation. The last term on the left includes wave radiation stress terms, $\overline{S}_{\alpha\beta}$, representing energy exchange with the mean velocity energy equation. The explicit record of the term is

$$\int_{-1}^{0}\overline{S}_{\alpha\beta}\frac{\partial U_\alpha}{\partial x_\beta}D\mathrm{d}\varsigma=E_\theta D\left[\cos^2\theta\int_{-1}^{0}\frac{\partial U}{\partial x}F_1\mathrm{d}\varsigma-\int_{-1}^{0}\frac{\partial U}{\partial x}F_2\mathrm{d}\varsigma+\cos\theta\sin\theta\int_{-1}^{0}\left(\frac{\partial U}{\partial y}+\frac{\partial V}{\partial x}\right)F_1\mathrm{d}\varsigma+\sin^2\theta\int_{-1}^{0}\frac{\partial V}{\partial y}F_1\mathrm{d}\varsigma-\int_{-1}^{0}\frac{\partial V}{\partial y}F_2\mathrm{d}\varsigma\right], \tag{11}$$

where $E_\theta=\int_0^\infty E_{\sigma,\theta}(x,y,t,\sigma,\theta)$ is the directional kinematic energy (divided by the water density), $E_\sigma=\int_{-\pi}^{\pi}E_{\sigma,\theta}\mathrm{d}\theta$, F_1=$E_{\mathrm{T}}^{-1}\int_0^\infty E_\sigma(k/k_p)F_{\mathrm{CS}}F_{\mathrm{CC}}\mathrm{d}\sigma$, F_2=$E_{\mathrm{T}}^{-1}\int_0^\infty E_\sigma(k/k_p)F_{\mathrm{SC}}F_{\mathrm{SS}}\mathrm{d}\sigma$ and $E_{\mathrm{T}}=\int_{-\pi}^{\pi}E_\theta\mathrm{d}\theta$; σ is the intrinsic frequency, k_p is the wave number where frequency is peak frequency; F_{CS}=$\cosh kD(1+\varsigma)/\sinh kD$, F_{CC}=$\cosh kD(1+\varsigma)/\cosh kD$, F_{SC}=$\sinh kD(1+\varsigma)/\cosh kD$, $F_{\mathrm{SS}}=\sinh kD(1+\varsigma)/\sinh kD$; θ is the wave propagation direction relative to the eastward direction, σ is the intrinsic frequency; $S_{\theta\mathrm{in}}$ is the wave energy source term dependent on wind properties. Thus, the atmospheric work done on the water is $\rho_w S_{\theta\mathrm{in}}$, where ρ_w is the sea water density. $S_{\theta\mathrm{Sdis}}$ and $S_{\theta\mathrm{Bdis}}$ are wave dissipation due to wave processes at the surface and bottom, respectively. The terms $\overline{c}_{g\alpha}$, $\overline{c}_\theta$, $\overline{u}_{\mathrm{A}\alpha}$ and $\overline{S}_{\alpha\beta}$ have been spectrally averaged. For more details on these variables, see ref. [13].

The spectrally averaged group speed is a function of frequency provided by

$$\frac{\partial\sigma_\theta}{\partial t}+(\overline{c}_{g\alpha}+\overline{u}_{\mathrm{A}\alpha})\frac{\partial\sigma_\theta}{\partial x_\alpha}=-\frac{\partial\sigma_\theta}{\partial k}\left(\frac{k_\alpha k_\beta}{k^2}\frac{\partial\overline{u}_{\mathrm{A}\alpha}}{\partial x_\beta}\right)+\frac{\partial\sigma_\theta}{\partial D}\left(\frac{\partial D}{\partial t}+\overline{u}_{\mathrm{A}\alpha}\frac{\partial D}{\partial x_\alpha}\right)+\sigma_p(\sigma_p-\sigma_\theta)f_{\mathrm{spr}}^{1/2}, \tag{12}$$

where $n=1/2+kD/\sinh 2kD$, $\partial\sigma_\theta/\partial D=(\sigma_\theta/D)(n-1/2)$, $\partial\sigma_\theta/\partial k=\overline{c}_g$, and $f_{\mathrm{spr}}=S_{\theta\mathrm{in}}/\int_{-\pi/2}^{\pi/2}S_{\theta\mathrm{in}}\mathrm{d}\theta$. In the regions of θ which is wind driven, σ_θ will be overwritten by the peak frequency σ_p provided by

$$\frac{E_{\mathrm{T}}g}{U_{10}^4}=0.0022\left(U_{10}\sigma_p/g\right)^{-3.3}, \tag{13}$$

which will determine σ_p as a function of $E_{\theta\max}$ and U_{10} for the wind driven portion of E_θ; for other portions of E_θ or for light or no winds, frequency is determined by eq. (12).

2.1.3 *Discretization and coupling procedure*

The flow module is solved numerically by the flux calculation in an integral form of eqs. (1)–(5), (8)–(10), and (12) over nonoverlapping, unstructured triangular grids. An unstructured triangle is composed of three nodes, a centroid, and three sides (Figure 3(a)), on which u, v, E_θ, c_θ, and σ_θ are placed at centroids and other scalar variables, such as η, H, D, ρ, w, C, K_{m}, K_{h}, A_{m} and A_{h}, are placed at nodes. Variables at each node are determined by the net flux through the sections linked to centroids and the middle point of the sideline in the surrounding triangles (dashed polygon shown in Figure 3(a)), while variables at centroids are calculated on the basis of the net flux through three sides of that triangle (bold triangle shown in Figure 3(a)). The angle space (Figure 3(b)) is from $-\pi$ to π, and is divided into MSEG bins, resulting in an angle increment of δ=

$2\pi/\text{mseg}$. Cyclic boundary conditions connect the branch cut at $-\pi$, π. Also the wave model is parallelized by using a METIS library [17]. A schematic diagram of cell-centered partitioning approach is shown in Figure 3(c). A second-order accuracy upwind finite difference scheme is used for flux calculation in the integral form of the advective terms, and the modified fourth-order Runge-Kutta time-stepping scheme is used for time integration. For more details about the discretization method, refer to refs. [13, 18].

A two-way dynamic coupling procedure is taken in this integrated model. Surface wind stress, bottom stress and 3-D radiation stress calculated in the wave model are provided to the hydrodynamic model. Contemporaneously, current fields and water surface elevation computed by the hydrodynamic model are provided to the wave model. The wave propagation time step usually can be the same as the internal time step of hydrodynamic model. Otherwise, for example, wave model will have to be called twice during one internal time step. This coupling procedure is illustrated in Figure 2.

2.2 Transport and fate module

The dispersion of oil is calculated by using a particle-tracking method. Essentially, the spilled oil on a sea surface is divided into a large number of small particles of equal mass under the influence of regular movement of the media with the velocity components $\langle u(x,y,z,t)\rangle$, $\langle v(x,y,z,t)\rangle$ and $\langle w(x,y,z,t)\rangle$, the buoyancy velocity of oil droplets u_{L} and the turbulent fluctuations $u'(x,y,z,t)$, $v'(x,y,z,t)$ and $w'(x,y,z,t)$. The coordinates X, Y and Z of oil particles can be determined by the following:

$$\begin{cases} \dfrac{\mathrm{d}X}{\mathrm{d}t} = \langle u\rangle + u', \\ \dfrac{\mathrm{d}Y}{\mathrm{d}t} = \langle v\rangle + v', \\ \dfrac{\mathrm{d}Z}{\mathrm{d}t} = \langle w\rangle + w' + u_{\mathrm{L}}, \end{cases} \tag{14}$$

where $\langle u\rangle$, $\langle v\rangle$ and $\langle w\rangle$ are drift velocities of oil particles which represent the drift due to the combined effect of the wind, current and waves on the surface layer as well as in the water column; u', v' and w' are the turbulent fluctuations of the velocity which simulate the turbulent diffusion of the oil droplets; u_{L} is the buoyancy velocity of oil droplets and is described below.

The drift velocity of the oil is the result of the combined action of wind, current and wave and can be written as follows [19]:

$$\begin{cases} \langle u\rangle = \alpha_w \boldsymbol{M}\, u_w + \alpha_c u_c + u_{\mathrm{wave}}, \\ \langle v\rangle = \alpha_w \boldsymbol{M}\, v_w + \alpha_c v_c + v_{\mathrm{wave}}, \\ \langle w\rangle = w_c, \end{cases} \tag{15}$$

where u_w, v_w are the wind velocities at 10 m above the water surface; u_c, v_c and w_c are the water current velocities; u_{wave} and v_{wave} are the wave-induced velocities; α_w is the wind drift factor, usually taken as 0.03 when the oil droplets are on the water surface or as zero if not; α_c is the factor to account for the contribution of the drift of the oil slick on the water surface due to the current and is selected as 1.1 while equal to 1.0 when in the water column. It may be noted that in the flow module $U = u_c + u_{\mathrm{wave}}$, $V = v_c + u_{\mathrm{wave}}$, so $\alpha_c u_c + u_{\mathrm{wave}}$, $\alpha_c v_c + v_{\mathrm{wave}}$ are replaced by $\alpha_c U$, $\alpha_c V$ for simplification. w_c is the velocity the oil particle locates, interpolated from the ς coordinate; $\boldsymbol{M}$ is the transformation matrix which allows introducing a deviation angle [19]:

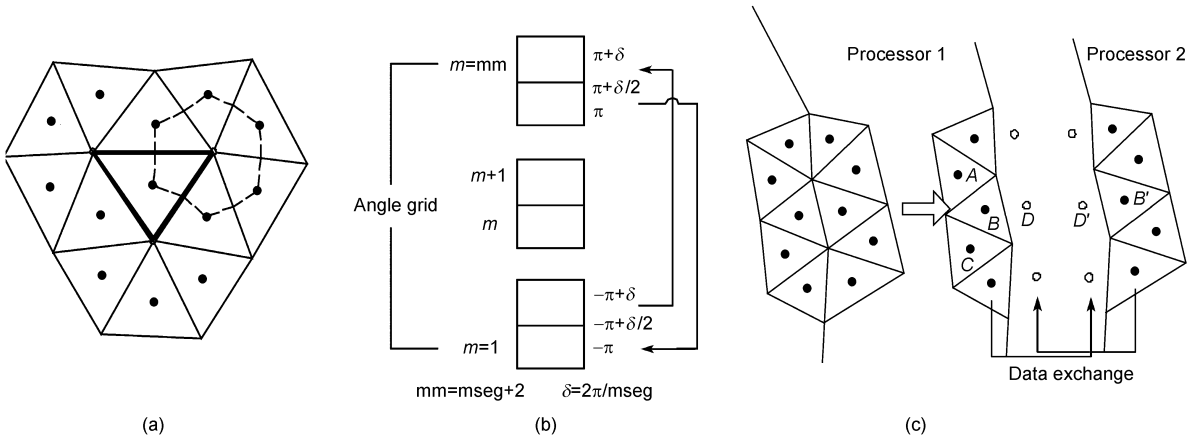

Figure 3 Schematic of the model grid. (a) Spatial unstructured grid; (b) propagation angle grid and the cyclic boundary conditions; (c) a schematic diagram of cell-centered partitioning approach.

$$\boldsymbol{M}=\begin{pmatrix}\cos\beta & \sin\beta\\ -\sin\beta & \cos\beta\end{pmatrix}, \tag{16}$$

where β=40°− $8\sqrt[4]{u_w^2+v_w^2}$ when $0\leqslant\sqrt{u_w^2+v_w^2}\leqslant 25$ m/s and β=0 when $\sqrt{u_w^2+v_w^2}$ >25 m/s.

The horizontal turbulent diffusive transport is generally calculated using a random walk technique. Based on Fischer et al.'s study [20], the fluctuation velocity components u' and v' are calculated as

$$\begin{cases}u'=\xi\sqrt{4A_{\mathrm{h}}/\Delta t}\sin(2\pi\phi),\\ v'=\xi\sqrt{4A_{\mathrm{h}}/\Delta t}\cos(2\pi\phi),\end{cases} \tag{17}$$

where ξ is a Gaussian random number with the unit intensity and the null mean value, ϕ is a uniform random in the interval of 0 to 1, and the value A_{h} is calculated directly from the flow module by Smagorinsky's formula.

The vertical diffusion process is formulated by solving the Langeven equation

$$\frac{\mathrm{d}w'}{\mathrm{d}t}=-\alpha w'(t)+\lambda\xi(t), \tag{18}$$

where the coefficients α and λ can be determined by the covariance and dispersion of the stochastic process $w'(t)$. The relationship between the Langeven equation and Markov's chain is

$$\begin{cases}w'(t+\Delta t)=\mathrm{e}^{(-\Delta t/T_{\mathrm{L}})}w'(t)+(1-\mathrm{e}^{(-2\Delta t/T_{\mathrm{L}})})^{1/2}\psi\xi(t)\\ \qquad\qquad +(1-\mathrm{e}^{(-\Delta t/T_{\mathrm{L}})})T_{\mathrm{L}}\dfrac{\partial\psi^2}{\partial z},\\ w'(0)=0,\end{cases} \tag{19}$$

where ψ is the r.m.s. value of velocity fluctuations; T_{L} is the Lagrange's integral time scale, defined as

$$\psi^2=c_0k,\quad T_{\mathrm{L}}=\frac{c_u}{c_0}\frac{k}{\varepsilon}, \tag{20}$$

where c_u=0.08 and c_0=0.3 are empirical constants which can be determined for each time provided with $k=q^2/2$ and $\varepsilon=1.35q^3/l$ from the flow module. Thus, eqs. (18) and (19) can reproduce vertical particle diffusion in the flow [6].

The oil slick on the ocean is also subject to the action of waves, especially breaking waves. The wind-driven breaking and non-breaking waves spilt the surface oil layer into droplets and then propel them into the water column. Using the model developed by Tkalich and Chan [21], the rate of oil entrainment from slick to the water column can be scaled as

$$\lambda_{ow}=\frac{\pi k_e\gamma H_s}{8\alpha TL_{ow}}, \tag{21}$$

where k_e is the coefficient evaluated from experiments, usually 0.3–0.5; $T=E_{\mathrm{T}}(\int_{-\pi}^{\pi}\sigma_\theta E_\theta\mathrm{d}\theta)^{-1}$ is the average wave period; γ is the dimensionless damping coefficient; $H_s=4(E_{\mathrm{T}}/g)^{1/2}$ is the significant wave height; α is coefficient concerning the mixing depth of the individual particles; L_{ow} is the vertical length-scale parameter, depending on the type of the breaking wave. Thus, the probability of the entrainment is calculated by

$$P_s=1-\exp(-\lambda_{ow}\Delta t), \tag{22}$$

and the intrusion depth was assumed as (1.35+0.35 $(3\phi$–1))H_s as suggested by Delvigne and Sweeney [22], where ϕ is a uniform random number between 0 and 1.

The buoyancy velocity of oil droplets is determined by their size, seawater viscosity and the density difference between seawater and oil droplets. The critical diameter of oil droplets is calculated by the following formula [23]:

$$d_c=\frac{9.52\cdot v^{2/3}}{g^{1/3}\cdot(1-\rho_{\mathrm{o}}/\rho)^{1/3}}. \tag{23}$$

For small oil droplets $d_i<d_c$, the Stokes law gives the steady buoyancy velocity

$$u_{\mathrm{L}}=gd_i^2(1-\rho_{\mathrm{o}}/\rho)/18v. \tag{24}$$

For big oil droplets $d_i\geqslant d_c$, the Reynolds law gives the steady buoyancy velocity

$$u_{\mathrm{L}}=\sqrt{\frac{8}{3}gd_i(1-\rho_{\mathrm{o}}/\rho)}, \tag{25}$$

where v is the seawater viscosity; ρ_{o} and ρ are the oil and seawater densities, respectively; d_i is the diameter of the oil droplet. Delvigne and Sweeney [22] conducted a series of laboratory investigations and found that the distribution of vertical diffusion oil droplets' diameters was a normally distributed random number with a mean value of 250 μm and a standard deviation of 75 μm.

Other factors, such as mechanical spreading, shoreline boundary conditions, evaporation, dissolution, and emulsification, which affect the spreading and motion of spilled oil slick, can be found in Wang et al. [10]. As the spilled oil is emulsified, its density, surface tension and viscosity may change; see Wang et al. [10] for details.

3 Application of the model to the oil spill accident in the Bohai Strait

A three-dimensional integrated oil spills model is developed based on the above analytical formulation and used to simulate the oil spill accident which occurred in the Bohai Strait.

Strait. The simulated results of the oil slicks after the spillage are presented and discussed.

3.1 Outline of the incident

On 8 June 1990, two ships collided in the Bohai Strait (38°32′48″N, 120°56′42″E) at 2:00 a.m. (Beijing time) with one seriously damaged and its tank broken. On 14 June, the amount of heavy fuel released continuously from the broken tank was estimated to be of the order of 250–350 t. At the same time, aerial surveys were carried out by a team of Chinese experts and the distribution of the spilled oil on the sea surface issued [19]. Some environmental factors observed by a monitoring vessel in the accident site indicated that the speed of wind, blowing from the south, did not exceed 4 m/s during those days. After 15 June, the oil spill continued but the survey had to be cancelled due to very bad weather conditions.

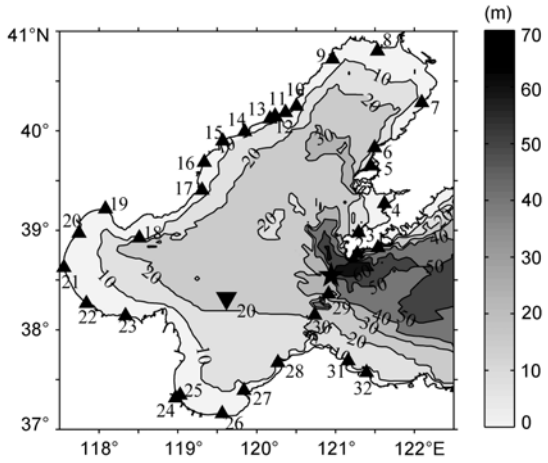

Figure 4 Model domain and bathymetry of the Bohai Sea (Numbers next to ▲ denote the tidal stations where tidal harmonic constants are compared between simulations and observations. ▼ denotes the tidal current observation station and ★ denotes the oil spill location).

3.2 Model setup and conditions

A high-resolution circulation model is required to describe the complex hydrodynamics of coastal areas of the Bohai Sea. The computational domain of this model, within 37°07′N–41°N latitude and 117°35′E–122.5°E longitude, is shown in Figure 4. To fit the irregular coastline better, the horizontal resolution should be about 1.5 km around the coast and about 7 km in the interior and near the open boundary; a refined grid is used around the oil spill location at the Bohai Strait. The computational grid is shown in Figure 5. In the vertical dimension the grid comprises 15 uniformly distributed σ layers. The model is driven by tidal forcing at the open boundary. The harmonic constants of M_2, N_2, S_2, K_2, K_1, O_1 and P_1 obtained from the coastal gauges at the northern and southern coasts were interpolated onto the open boundary. The climatological temperature and salinity derived from ref. [24] (hereafter referred to as "the atlas") are used as our model initial conditions. At the sea surface, the model is forced by monthly climatological SST and SSS, respectively. The monthly climatological wind field derived from the QuickSCAT sea surface vector winds is used to drive the model. The external and internal mode time steps were 10.0 and 180.0 s. The model is spun up as of 1 January 1989 until the time of the oil-spill accident, then the wind speed is changed to 3 m/s in an SSW direction, and another 8 days are simulated to provide the hydrodynamic parameters to the transport-fate module.

Since the transport-fate module was designed in a z-level coordinate system, the simulated velocity and diffusivity data from flow module were converted from sigma levels to z-levels, and linear interpolation between the two types of levels was implemented. The transport module had 140 vertical levels; the vertical resolution was 0.5 m. In the horizontal, the two modules share the same resolution.

The simulation time of the transport-fate module is 8 days,

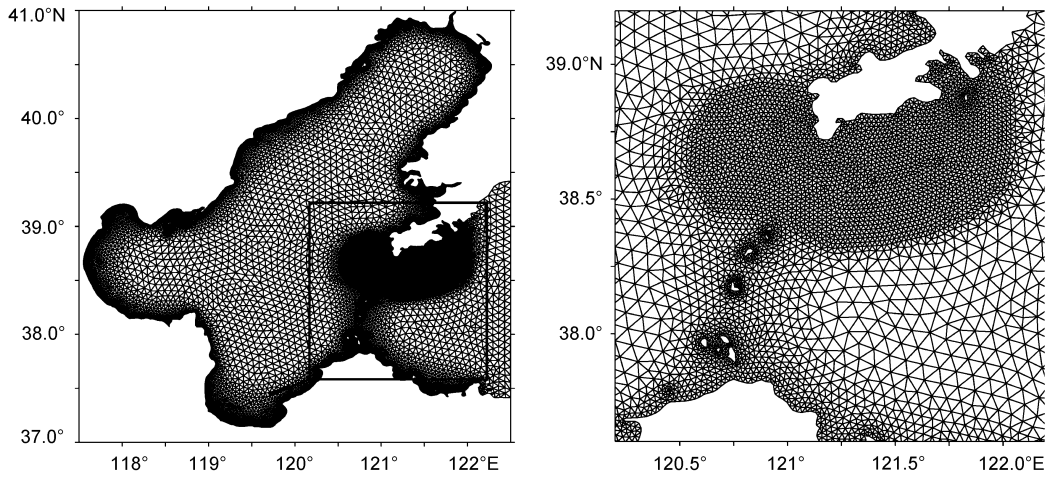

Figure 5 Unstructured grid of the flow module (The right panel provides an enlarged view of the grid around the oil spill location).

starting from 8 June 1990 at 2:00 when the accident happened. During this time 5760 oil particles were released. It is assumed from the observations that a continuous release of six days is reasonable. The time interval between two releases was set as 1 h, with 40 oil particles released each time. The input data are summarized in Table 1.

3.3 Results and discussion

Model-predicted amplitudes and phases of tidal elevation and tidal current were output at each vertex of a triangle and calibrated using the existing tidal observational data. Computed tidal charts for the M_2 and K_1 tides are presented in Figure 6. The cotidal chart lines are in good agreement with the atlas. A comparison of tidal harmonic constants at 32 stations between model results and observations indicates a good reproduction of the four major tidal constituents in the Bohai Sea (Figure 7). The tidal ellipse charts show that the tidal current reaches its maximum speed at about 38°50′N, 121°E. This location roughly coincides with the place of the accident, indicating that tidal current may exert a significant effect on spreading the spilled oil.

A comparison between computed and current amplitudes and phases deduced from measurements [25] at the current observation station can be seen in Table 2. The agreement in currents is good except for the K_1, O_1 currents at the bottom. It should be noted that the measurement uncertainty is not considered. The wave parameters, including significant wave height and mean wave period at the beginning of the spill, are shown in Figure 8.

Table 1 Input parameters for sample simulations

Simulation time (d)	Spill time step Δt (min)	Oil particle number N_0	Sea bed deposition coefficient (s^{-1})	Emulsification coefficient (s^{-1})
8	12	5760	10^{-5}	10^{-6}
Resurfacing coefficient	Buoyant velocity (m/s)	Air temperature (°C)	Water viscosity (m^2/s)	Total spilled volume (m^3)
1.0	0.00254	10.0	1.311×10^{-6}	300.0
Oil type	Ice cover condition	Wind velocity	Spill location	Spill condition
Heavy fuel (sp. gr.=0.965)	Open water	0–192 h, 3.0 m/s from SSW	(38°32′48″N, 120°56′42″E)	Continuous spill, duration=6 d
Oil viscosity (m^2/s)	Surface tension (N/m)	Evaporation parameters C	Solubility parameter α (d^{-1})	Solubility parameter KS_0 ($g^{-2}\cdot h^{-1}$)
8.6×10^{-4}	0.02	7.88	0.423	0.0184

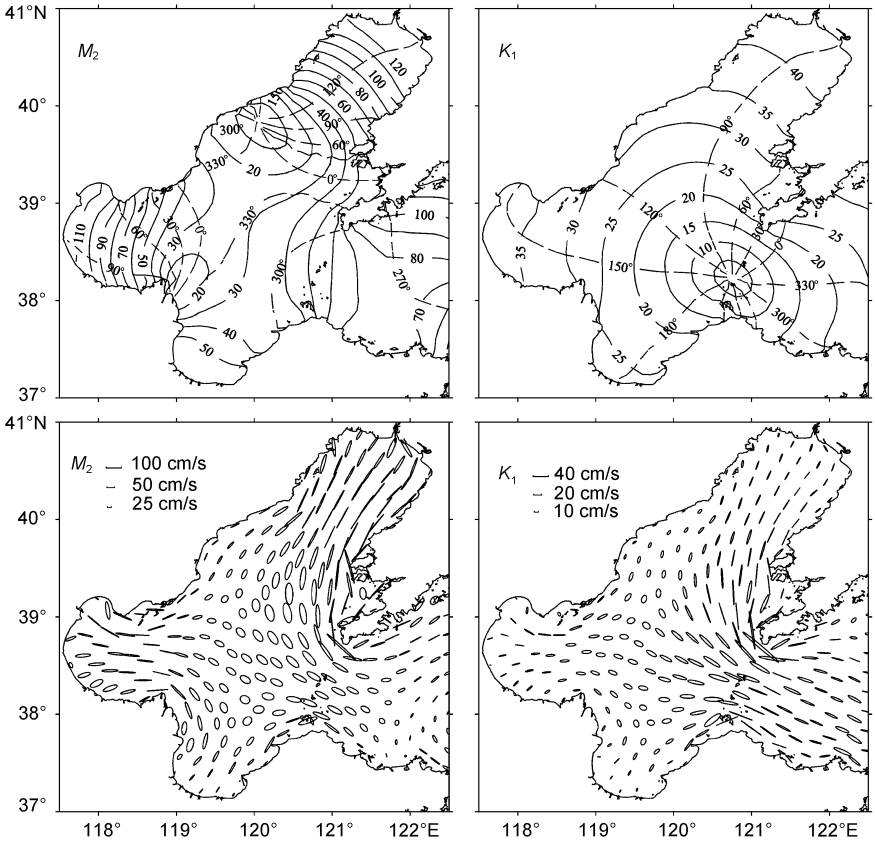

Figure 6 Co-amplitude line (solid, in cm) and co-phase line (dashed, in degree) of M_2 and K_1 (upper panels) and their tidal current ellipses (lower panels).

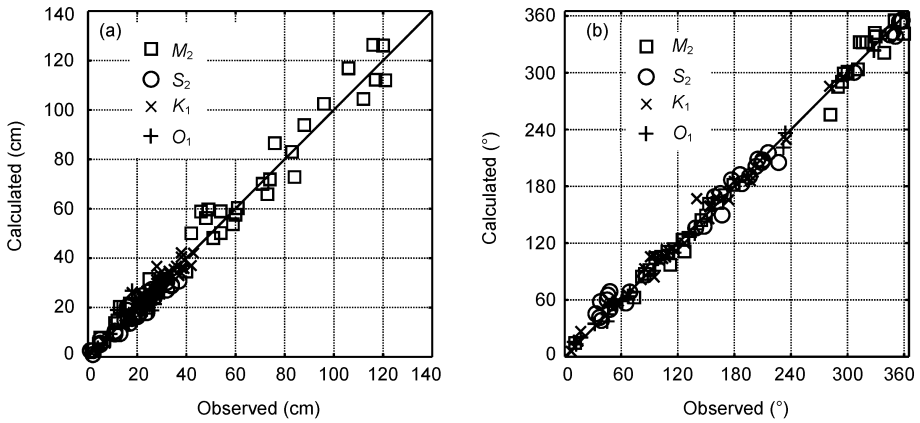

Figure 7 Comparison of harmonic constants derived from simulations (ordinate) and observations (abscissa) at 32 tidal stations as shown in Figure 4 for (a) amplitude and (b) phase (Different symbols denote different tidal constituents).

Table 2 Comparison between model-calculated and observed tidal current harmonic constants at the current observation station (38°19′39.426″N, 119°37′1.546″E, H_U, G_U are amplitude and phase lag of northern current component; H_V, G_V are amplitude and phase lag of eastern current component)

		H_U (cm/s)		G_U (°)		H_V (cm/s)		G_V (°)	
		Observed	Calculated	Observed	Calculated	Observed	Calculated	Observed	Calculated
Surface	M_2	20.11	22.18	45.51	43.80	31.13	30.88	176.50	169.98
	S_2	4.79	4.94	122.34	131.98	7.38	7.39	236.41	250.65
	K_1	7.03	4.57	49.87	38.60	14.22	12.50	224.70	236.07
	O_1	6.32	4.15	13.94	358.41	8.73	7.48	189.43	171.97
Bottom	M_2	16.85	15.06	15.46	35.72	25.88	22.78	156.52	165.66
	S_2	4.29	3.14	89.10	115.90	7.23	5.32	214.42	237.30
	K_1	3.22	3.39	52.74	66.15	16.52	10.24	238.84	231.27
	O_1	4.16	2.74	53.37	78.53	13.37	5.62	204.91	169.47

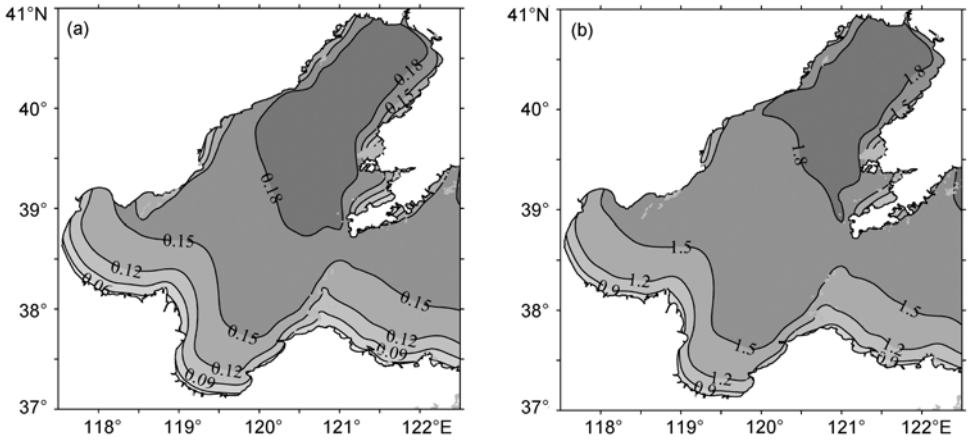

Figure 8 (a) Simulated significant wave height (unit: m) and (b) averaged wave period (unit: s) at the beginning of the oil spill.

Figures 9(a) and (b) are the observed distributions of the spilled oil slick on 12 and 15 June, respectively. Figures 10(a) and (b) are the simulated distributions of the oil slick on 12 and 15, respectively. Comparing Figures 10(a) and (b) reveals an eastward movement of the simulated oil slick, which agrees with the main tendency of the spreading of the observed oil slick (see Figure 9). Also, the map of oil concentrations, computed from the density of particles per water volume unit, is presented in Figure 11. It can be seen that the center of the spill mass moves to 121.05°E, 38.45°N with the highest concentration about 1.4 mg/L until 12 June, moving along a northeasterly direction to 121.2°E, 38.52°N,

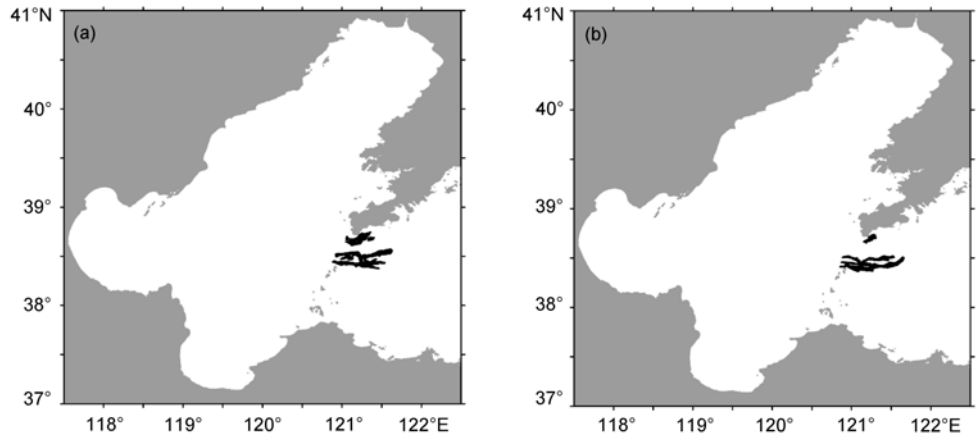

Figure 9 Snapshots showing the distributions of oil slick observed. (a) On 12 June; (b) on 15 June.

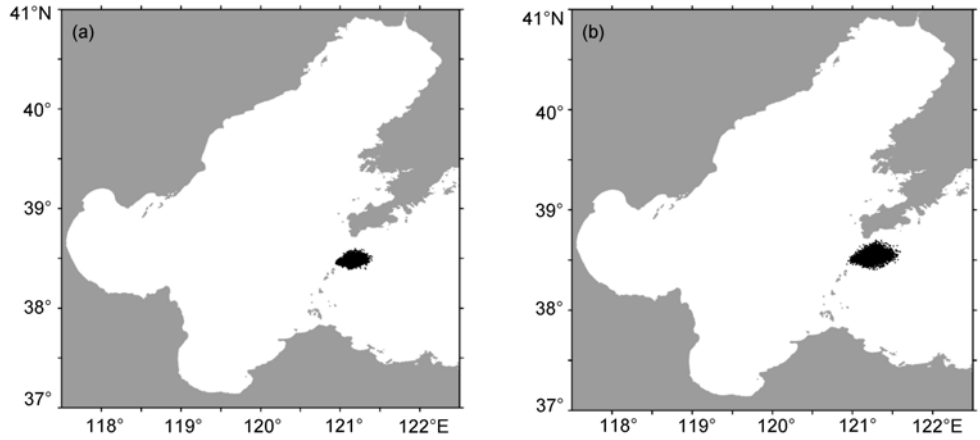

Figure 10 Snapshots showing the distributions of oil slick simulated. (a) On 12 June; (b) on 15 June.

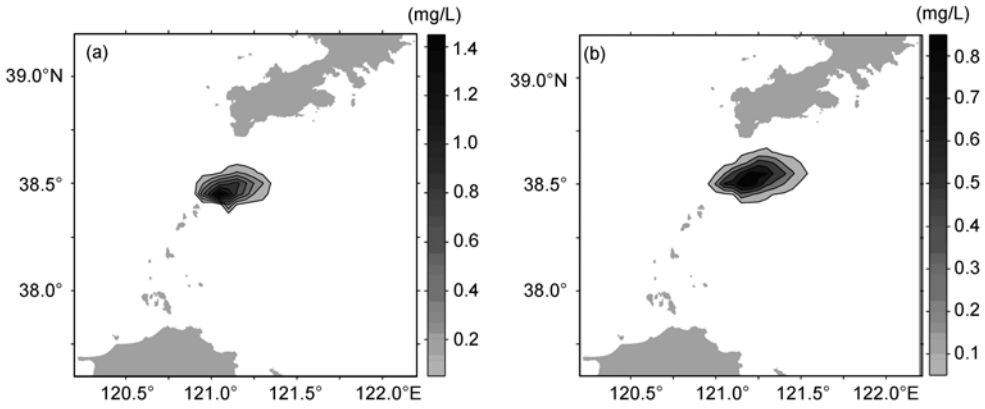

Figure 11 The computed oil concentrations. (a) On 12 June; (b) on 15 June.

with the highest concentration about 0.85 mg/L until 15 June.

The simulated vertical distributions of oil droplets are presented in Figure 12. Under the action of surface waves, particles have a preference for entraining in the water column. The turbulent mixing force may propel a few oil particles deeper into the water column. Owing to the effect of buoyancy, most particles will resurface. Unfortunately, there was no observed vertical distribution of an oil slick for comparison. Nevertheless, this result is reasonable according to the observed vertical distribution of air bubble [26].

Figure 13 summarizes the computed oil fate as a time

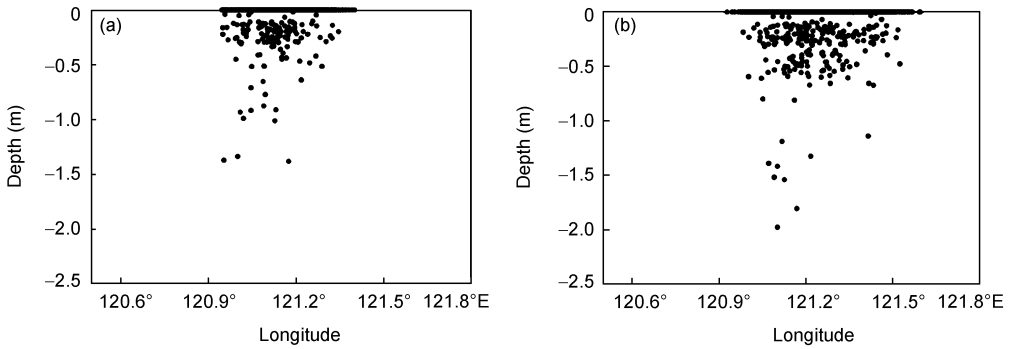

Figure 12 The vertical distributions of oil droplets simulated in the water column. (a) On 12 June; (b) on 15 June.

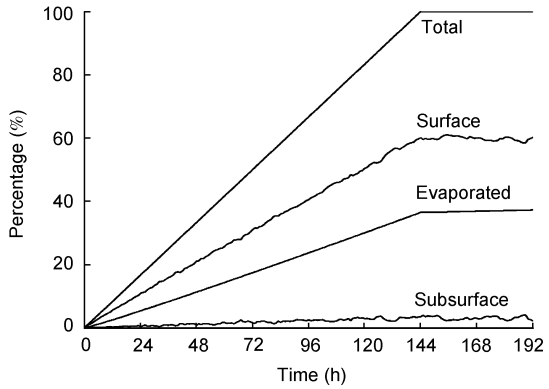

Figure 13 Time series of modeled oil components.

history of oil emitted, oil evaporated, and oil dispersed below the surface with an SSW wind of 3 m/s. As is seen, evaporation is the primary initial process involved in the removal of oil from the sea, i.e., more than 35%. With a gentle breeze, only about 3.5% of the oil is dissolved and dispersed in the water column. There remains 60% of total oil on the surface until the end of the simulation.

Thus it seems that, generally speaking, even with rather poor information about wind conditions provided, the present model can at least give a first-order prediction of the oil-slick displacement. With improvement in the reliability of external information, such as wind conditions, better simulated results might be achieved.

4 Conclusions

The description of an integrated three-dimensional model for simulating oil-spill transport and fate in seas has been presented in this paper. The transport-fate module is based on the particle approach. The amount of oil released at sea is distributed among a large number of particles tracked individually. These particles move in a 3-D space. They are driven by water currents, wave- and wind-induced speed when they are on the water's surface, whereas they move vertically in the water column owing to buoyancy. Horizontal diffusion is simulated using a random walk technique, whereas vertical diffusion processes are solved on the basis of the Langeven equation. Three weathering processes, emulsification, dissolution and evaporation, which modify the characteristics of the surface oil, have been simulated.

An unstructured finite-volume parallel wave-ocean model is developed as the flow module to provide the hydrodynamic parameters to the transport-fate module. Using unstructured meshes provides great flexibility for modeling the flow in arbitrary and complex geometries, such as those of the Bohai Strait domain. Moreover, a surface-wave model is coupled with the ocean model. This coupling includes depth-dependent wave-radiation-stress terms, Stokes' drift, vertical transfer of wave-generated pressure to the mean-momentum equation, wave dissipation as a source term in the turbulence kinetic-energy equation and mean current advection and refraction of wave energy.

The integrated model has been applied to an oil-spill accident that took place in the Bohai Strait (China). The flow module has been validated through the comparison of computed tidal elevations, phases and currents with measurements in the area. Results are in good agreement with observations. The simulated trajectories of the spilled oil slick were similar to the observed movement tendency of the slick, although rather poor wind data were provided. It should be noted that the simulated results could be improved if more accurate environmental data were provided. Further model validation by means of laboratory/field environmental data and integrate water quality model [27] should be taken into account in the future. Generally speaking, the simulated results show that the model is useful for investigating the behavior of oil spills in an area of complex geography. This model can be used as a tool for estimating the impact of spilled oil on the marine environment, thereby providing useful information to assist spill response after a paroxysmal oil accident.

This work was supported by the National Natural Science Foundation of China (Grant No. 50839001), the National Basic Research Program of China ("973"Program)(Grant No. 2005CB724202) and the Scientific Research Foundation of the Higher Education Institutions of Liaoning Province (Grant No. 2006T018).

1 Elliott A J. Shear diffusion and the spread of oil in the surface layers of the North Sea. Ocean Dynam, 1986, 39(3): 113–137
2 Periáñez R, Pascual-Granged A. Modelling surface radioactive, chemical and oil spills in the Strait of Gibraltar. Comput Geoscien, 2008, 34(2): 163–180
3 Wang S D, Shen Y M, Guo Y K, et al. Three-dimensional numerical simulation for transport of oil spills in seas. Ocean Eng, 2008, 35(5-6): 503–510
4 Chao X B, Shankar N J, Cheong H F. Two- and three-dimensional oil spill model for coastal waters. Ocean Eng, 2001, 28(12): 1557–1573
5 Chao X B, Shankar N J, Wang S. Development and application of oil spill model for Singapore coastal waters. J Hydraul Eng-ASCE, 2003, 129(7): 495–503
6 Lonin S A. Lagrangian model for oil spill diffusion at sea. Spill Sci T, 1999, 5(5): 331–336
7 Shen H T, Yapa P D. Oil slick transport in rivers. J Hydraul Eng-ASCE, 1988, 114(5): 529–543
8 Shen H T, Yapa P D, Petroski M E. Simulation of Oil Slick Transport in Great Lakes Connecting Channels. Technical Report, Department of Civil and Environmental Engineering, Clarkson University. 1986
9 Yapa P D, Shen H T, Angammana K S. Modeling oil-spills in a river lake system. J Marine Syst, 1994, 4(6): 453–471
10 Wang S D, Shen Y M, Zheng Y H. Two-dimensional numerical simulation for transport and fate of oil spills in seas. Ocean Eng, 2005, 32(13): 1556–1571
11 Periáñez R. Chemical and oil spill rapid response modelling in the Strait of Gibraltar–Alborán Sea. Ecol Model, 2007, 207(2-4): 210–222
12 Chen C S, Huang H S, Beardsley R C, et al. A finite volume numerical approach for coastal ocean circulation studies: Comparisons with finite difference models. J Geophys Res, 2007, 112: C3018, doi: 10.1029/2006JC003485
13 Mellor G L, Donelan M A, Oey L Y. A surface wave model for coupling with numerical ocean circulation models. J Atmos Ocean Tech, 2008, 25(10): 1785–1807
14 Mellor G L. Some consequences of the three-dimensional current and surface wave equations. J Phys Oceanogr, 2005, 35(11): 2291–2298
15 Blumberg A F, Mellor G L. A description of a three-dimensional coastal ocean circulation model. In: Heaps N, ed. Three-Dimensional Coastal Ocean Models. Washington: American Geophysics Union, 1987. 1–16
16 Mellor G L. The three-dimensional current and surface wave equations. J Phys Oceanogr, 2003, 33(9): 1978–1989
17 Karypis G, Kumar V. Metis: A Software Package for Partitioning Unstructured Graphs, Partitioning Meshes, and Computing Fill-Reducing Orderings of Sparse Matrices. Technical Report, Department of Computer Science, University of Minnesota. 1998
18 Chen C S, Liu H D, Beardsley R C. An unstructured grid, finite-volume, three-dimensional, primitive equations ocean model: Application to coastal ocean and estuaries. J Atmos Ocean Tech, 2003, 20(1): 159–186
19 Zhang B, Zhang C Z, Ozer J. Surf–a simulation model for the behavior of oil slicks at sea. In: Ozer J, ed. Oil Pollution: Environmental Risk Assessment (OPERA). Belgium: Caligrafic Dewarichet, 1991. 61–85
20 Fischer H B, List E J, Koh R, et al. Mixing in Inland and Coastal Waters. New York: Academic Press, 1979
21 Tkalich P, Chan E S. Vertical mixing of oil droplets by breaking waves. Mar Pollut Bull, 2002, 44(11): 1219–1229
22 Delvigne G, Sweeney C E. Natural dispersion of oil. Oil Chem Pollut, 1988, 4(4): 281–310
23 Proctor R, Flather R A, Elliott A J. Modelling tides and surface drift in the Arabian Gulf: Application to the gulf oil spill. Cont Shelf Res, 1994, 14(5): 531–545
24 Editorial Board for Marine Atlas. Marine Atlas of the Bohai Sea, Yellow Sea and East China Sea: Hydrology (in Chinese). Beijing: China Ocean Press, 1992
25 Qiao L L, Bao X W, Wu D X. The observed currents in summer in the Bohai Sea. Chin J Limnol Oceanogr, 2008, 26(2): 130–136
26 Thorpe S A. On the clouds of bubbles formed by breaking wind-waves in deep water, and their role in air-sea gas transfer. Philos Trans R Soc London (A), 1982, 304(1483): 155–210
27 Shen Y M, Li Y C, Chwang A T. Quasi-three-dimensional refined modelling of turbulent flow and water quality in coastal waters. Sci China Ser E-Tech Sci, 1996, 39(4): 342–353